AIMS Mathematics, 11(5): 14239–14252.
DOI:10.3934/math.2026584
Received: 13 February 2026
Revised: 22 April 2026
Accepted: 07 May 2026
Published: 19 May 2026

https://www.aimspress.com/journal/Math

*Research article*

# Ruled surfaces as wave fronts in Galilean space $\mathbb{G}_3$ and characterizations of geometric singularities

**Ümit Tokeşer*** **and Seda Nur Ídrísoğlu**

Department of Mathematics, Faculty of Science, Kastamonu University, Kastamonu 37100, Turkey

* **Correspondence:** Email: utokeser@kastamonu.edu.tr.

**Abstract:** The aim of this study is to obtain a general version of constant-angle ruled surfaces constructed using a Frenet frame in Galilean space $\mathbb{G}_3$. We define generalized special ruled surfaces by considering cases where the surface normal vectors are parallel to the tangent, principal normal, or binormal vector fields of the base curve. We provide criteria regarding the locus of singular points of these surfaces. Specifically, for a general constant angle ruled surface whose normal vectors are parallel to the binormal vector field ($\mathcal{M}^b$), we explicitly characterize the singular set as $\{(s, -\upsilon(s)/\delta_1(s)\kappa(s)) : s \in I\}$. We establish analogous singular sets and characterizations for cuspidal edge, swallowtail, and cuspidal butterfly singularities for a surface whose normal vectors are parallel to the tangent vector field ($\mathcal{M}^t$). Conversely, we conclude that the general constant angle ruled surface whose normal vectors are parallel to the principal normal vector field. ($\mathcal{M}^n$) has no singular points. Finally, as an application of the findings, we give some illustrated examples of helices with singularities.

**Keywords:** helix; striction curve; singularities; Galilean 3-space
**Mathematics Subject Classification:** 53A35, 53A40, 57R45

## 1. Introduction

A helix is a curve that winds around an axis or a solid structure in three -dimensional space such as nanosprings; carbon nanotubes; $\alpha$-helices; DNA double and collagen triple helices; bacterial flagella in salmonella and escherichia coli; aerial hyphae in actinomycetes; bacterial shape in spirochetes, horns, tendrils, vines, screws, springs and helical staircases; and seashells [1–3]. Furthermore, hyperhelices were defined as the helix curve or helical structures in fractal geometry [4]. Moreover, helices can be used for the tool path description of any kinematic motion which was designed by computer simulation [5].

A Galilean space can be defined as the limit case of a pseudo-Euclidean space where the isotropic

cone degenerates to a plane. Thus, this limit transition corresponds to the limit transition from the special theory of relativity to classical mechanics. On the other hand, Galilean space-time plays an important role in nonrelativistic physics, as well as fundamental concepts and principles in classical physics such as velocity, momentum, kinetic energy, laws of motion, and gravitational laws, which are expressed in terms Galilean space [6].

Previous research has investigated the position vectors of curves in the Galilean space $\mathbb{G}_3$ by using the position vector of an arbitrary curve in Galilean 3-space. For this, the position vector of an arbitrary curve was first determined concerning the Frenet frame. Moreover, some special curves having the position vectors were obtained and sketched, defining a plane curve, helix, general helix, and Salkowski and anti-Salkowski curves in Galilean space $\mathbb{G}_3$ [7].

The explicit parameter equations of $T$-slant helices were obtained by defining $T$-slant, $N$-slant, and $B$-slant helices in Galilean space $\mathbb{G}_3$. It was proven that an admissible curve is a $T$-slant helix with a nonisotropic axis if and only if it has a nonzero constant conical curvature. In the pseudo-Galilean space $\mathbb{G}_3^1$, $T$-slant, $N$-slant, and $B$-slant helices were studied by defining an angle between the spacelike and the timelike isotropic vector lying in the pseudo-Euclidean plane $x = 0$. The explicit parameter equations belonging to the $T$-slant helices were obtained. It was found that there are no $N$-slant, $B$-slant, and Darboux helices in $\mathbb{G}_3$ and in $\mathbb{G}_3^1$ [8, 9]. In other studies, characterizations of the helix for a curve were obtained with respect to the Frenet frame in 3-dimensional Galilean space $\mathbb{G}_3$ [10].

In Euclidean space $\mathbb{E}^3$, a regular curve is called the general helix and the slant helix in two types. Whereas the tangent vector $T$ makes a constant-angle with some fixed direction for the general helix, the principal normal vector $N$ makes a constant-angle with the fixed direction for the slant helix [9]. A constant geodesic curvature of the spherical image of their principal normal indicatrix for slant helices was found. There are studies about some characterizations of the slant helices, and curves as Darboux helices in $\mathbb{E}^3$ where the Darboux vector makes a constant angle with some fixed direction were defined. Additionally, Darboux helices have been studied in Minkowski space $\mathbb{E}^3$. Some characterizations of general helices were also studied [11–13]. In 2018, Alghanemi and Alofi [14] studied the singularities of $M_{BT}$ and $M_{TB}$ surfaces and presented the geometric conditions for them to have certain singularities such as cuspidal edge, swallowtail, and cuspidal butterfly singularities.

The study of ruled surfaces in modern differential geometry, particularly within Euclidean and Minkowski ($E_1^3$) spaces, has moved beyond traditional methods to focus on more dynamic and "rotation-minimizing" frames. The research conducted by Emad Solouma and his collaborators [15–17] demonstrated that employing frames such as the rotation-minimizing (RM) Darboux, Bishop, and Hasimoto frames is critical for characterizing these surfaces. These frameworks allow for a deeper analysis of geometric invariants, harmonic evolutions, and singularity points. Such modern approaches provide a more flexible and precise mathematical foundation for the curvature analysis of imbricate-ruled and osculating type-2 surfaces under Lorentzian structures, which are essential for relativistic models and theoretical physics applications. As a more technical detail, the RM Darboux frame used in these studies eliminates unnecessary rotation in the normal vector field of a curve on the surface. This allows the evolution of the surface geometry to be expressed through much simpler and more elegant equations [18–20].

According to the study about the singularities of Galilean height functions concerning the Frenet frame along a curve embedded into Galilean space $\mathbb{G}^3$ [21], the relationships were obtained between singularities of discriminant and bifurcation sets of the function and geometric invariants of curves in

Galilean space. Because singularity theory is related to geometry in differential calculus, the theory is relevant to all the branches of mathematics, physics, and other disciplines, which concern geometry.

In this study, we introduce the constant-angle ruled surfaces in Galilean space $\mathbb{G}_3$ generated by a Frenet frame and investigate certain singularities in terms of the properties of cuspidal edges, swallowtail, and cuspidal butterfly singularities.

## 2. Basic concepts and background

The Galilean space is a Cayley-Klein space equipped with the projective metric of signature $(0, 0, +, +)$. The absolute figure of the Galilean geometry consists of an ordered triple $\{\omega, f, I\}$, where $\omega, f$, and $I$ are the real (absolute) plane, the real line (absolute line) in $\omega$, and the fixed hyperbolic involution of points of $f$, respectively [5]. In the Galilean space $\mathbb{G}_3$, there are four classes of lines:

- (proper) nonisotropic lines—lines that do not meet the absolute line $f$,
- (proper) isotropic lines—lines that do not belong to the plane $\omega$ but meet the absolute line $f$,
- (unproper) nonisotropic lines—all lines of $\omega$ but $f$,
- the absolute line $f$.

A plane is called Euclidean if it contains $f$; otherwise, isotropic, that is planes $x = const.$ are Euclidean, and so is the plane $\omega$. Other planes are isotropic.

In nonhomogenous coordinates, the similarity group $H_8$ has the following form:

$$\begin{aligned} \tilde{x} &= a_{11} + a_{12}x, \\ \tilde{y} &= a_{21} + a_{22}x + a_{23}\cos\theta y + a_{23}\sin\theta z, \\ \tilde{z} &= a_{31} + a_{32}x - a_{23}\sin\theta y + a_{23}\cos\theta z, \end{aligned}$$

where $a_{ij}$ and $\theta$ are real numbers [6]. The Galilean scalar product between two vectors $\sigma = (\sigma_1, \sigma_2, \sigma_3)$ and $\rho = (\rho_1, \rho_2, \rho_3)$ in the Galilean space $\mathbb{G}_3$ is defined by

$$\langle \sigma, \rho \rangle = \begin{cases} \sigma_1\rho_1, & \text{if } \sigma_1 \text{ or } \rho_1 \text{ is not zero,} \\ \sigma_2\rho_2 + \sigma_3\rho_3, & \text{if } \sigma_1 \text{ and } \rho_1 \text{ are zero,} \end{cases} \tag{1}$$

and the Galilean cross product is given as follows:

$$(\sigma \times \rho) = \begin{cases} \begin{vmatrix} 0 & e_2 & e_3 \\ \sigma_1 & \sigma_2 & \sigma_3 \\ \rho_1 & \rho_2 & \rho_3 \end{vmatrix} & \text{if } \sigma_1 \text{ or } \rho_1 \text{ is not zero,} \\ \begin{vmatrix} e_1 & e_2 & e_3 \\ \sigma_1 & \sigma_2 & \sigma_3 \\ \rho_1 & \rho_2 & \rho_3 \end{vmatrix} & \text{if } \sigma_1 \text{ and } \rho_1 \text{ are zero [7].} \end{cases} \tag{2}$$

Let $\gamma : I \subset \mathbb{R} \to \mathbb{G}_3$, $\gamma(u) = (x(u), y(u), z(u))$ be an admissible curve with the Galilean invariant parameter $s$. If $x(u)$ is considered as the arc length parameter of the curve, we get the curve as $\gamma(u) = (u, y(u), z(u))$. Then, the curvature $\kappa(u)$ and the torsion $\tau(u)$ of the curve $\gamma$ are defined by

$$\begin{aligned} \kappa(u) &= \sqrt{(y'')^2(u) + (z'')^2(u)}, \\ \tau(u) &= \frac{\det\left(y'(u), y''(u), y'''(u)\right)}{(\kappa(u))^2}, \end{aligned} \tag{3}$$

and the associated moving trihedron is given by

$$\begin{array}{ll} t(u) & = \gamma'(u) = (1, y'(u), z'(u)), \\ n(u) & = \frac{1}{\kappa(u)}(0, y''(u), z''(u)), \\ b(u) & = \frac{1}{\kappa(u)}(0, -z''(u), y''(u)). \end{array} \tag{4}$$

The vectors $t, n, b$ are called the vectors of the tangent, principal normal, and binormal line, respectively. The frenet equations of the curve $\gamma(u)$ are given by

$$\frac{d}{du}\begin{bmatrix} t \\ n \\ b \end{bmatrix} = \begin{bmatrix} 0 & \kappa & 0 \\ 0 & 0 & \tau \\ 0 & -\tau & 0 \end{bmatrix}\begin{bmatrix} t \\ n \\ b \end{bmatrix}, \tag{5}$$

where

$$\begin{array}{lll} t \times n = b, & t \times t = 0, & n \times t = -b, \\ n \times b = (1,0,0), & n \times n = 0, & b \times n = (-1,0,0), \\ b \times t = \left(0, \frac{y''}{\kappa}, \frac{z''}{\kappa}\right), & b \times b = 0, & t \times b = \left(0, -\frac{y''}{\kappa}, -\frac{z''}{\kappa}\right) \text{ [7].} \end{array} \tag{6}$$

The direction of such an axis is given by a Darboux vector which is expressed by the equation

$$\mathcal{D}(s) = \tau(s)t(s) + \kappa(s)b(s). \tag{7}$$

By using the Darboux vector, the Frenet formulas can be rewritten as follows:

$$\begin{array}{lll} \mathcal{D}(s) \times t(s) & = & t'(s), \\ \mathcal{D}(s) \times n(s) & = & n'(s), \\ \mathcal{D}(s) \times b(s) & = & b'(s), \end{array} \tag{8}$$

where $\times$ is the wedge product in Galilean space $\mathbb{G}_3$.

A ruled surface in the Galilean space $\mathbb{G}_3$ is a surface that admits a parametrization

$$\Phi(u, v) = \alpha(u) + va(u), \tag{9}$$

where $\gamma$ is an admissible curve (the directrix); $a$ is a nowhere vanishing vector field (field of generators) along the curve $\gamma$; and $u, v$ are parameters, $u \in I \subset \mathbb{R}$, $v \in \mathbb{R}$. In Galilean space $\mathbb{G}_3$, there are three types of ruled surfaces as follows:

*TYPE A*. Nonconodial or conodial ruled surfaces whose striction line does not lie in a Euclidean plane;

*TYPE B*. Ruled surfaces with the striction line in a Euclidean plane;

*TYPE C*. Conodial ruled surfaces with the absolute line as the directional line in infinity [13].

A ruled surface of type $A$ in Galilean space $\mathbb{G}_3$ can be parametrized by

$$\Phi_A(u, v) = \gamma(u) + va(u), \tag{10}$$

where the curve $\gamma(u) = (u, y(u), z(u))$, called an *admissible curve*, does not lie in a Euclidean plane and the generators $a(u) = (1, a_2(u), a_3(u))$ are *nonisotropic*.

**Definition 1.** *Let $\gamma$ be a unit speed regular curve in Galilean space $\mathbb{G}_3$, and $\{T, N, B\}$ be the Frenet frame in Galilean space $\mathbb{G}_3$ along $\gamma$. A curve $\gamma$ such that*

$$\frac{\kappa}{\tau} = const.$$

*is called* a general helix *with respect to the Frenet frame [10].*

**Definition 2.** *Let $\gamma$ be a unit speed regular curve in Galilean space $\mathbb{G}_3$, and $\{T, N, B\}$ be the Frenet frame in Galilean space $\mathbb{G}_3$ along $\gamma$. If $\kappa$ and $\tau$ are positive constants along $\gamma$, then $\gamma$ is called* a circular helix *with respect to the Frenet frame [10].*

**Definition 3.** *A ruled surface is a smooth one-parameter family of lines. Thus, a ruled surface $\mathcal{M}$ in $\mathbb{G}_3$ admits the parametrization:*

$$\mathcal{M} : U \subset \mathbb{R}^2 \to \mathcal{M} \subset \mathbb{G}_3, \mathcal{M}(s, u) = \gamma(s) + u\delta(s),$$

*where the curve $\gamma$ is called a* directrix *or* base curve *(with the condition regular) of the ruled surface, and $\delta$ denotes the* director curve. *The rulings of the ruled surface are the straight lines. A noncylindrical ruled surface has a parameterization of the form*

$$\overline{\mathcal{M}}(s, u) = \beta(s) + u\delta(s),$$

*where $\|\delta(s)\| = 1$, and $d/ds\,(\beta(s)) \times d/ds\,(\delta(s)) = 0$. Then, the curve $\beta$ is called the* striction curve *of $\mathcal{M}$.*

## 3. General constant angle ruled surfaces and their singularities

It is important to note that these general constant-angle ruled surfaces (GCARS) correspond to the constant-angle ruled surfaces (CARS) given in [22] for the well-known Serret-Frenet formulas of a base curve in $\mathbb{E}^3$. In this section, we first provide a general representation of GCARS that are parallel to specific special vectors along the base curves. Subsequently, we investigate the singularities of some special GCARS along with illustrative examples.

**Definition 4.** *Let $\gamma : I \subset \mathbb{R} \to \mathbb{G}_3$ be a unit speed regular curve in $\mathbb{G}_3$ and $\{t(s), n(s), b(s)\}$ be its moving Frenet frame. Let $U$ be a nonzero constant vector field in $\mathbb{G}_3$.*

*i) $\gamma$ is called a t-helix if the Galilean scalar product of its tangent vector field $t(s)$ and the constant vector $U$ remain constant for all $s \in I$, that is $\langle t(s), U\rangle = c_1$ for some constant $c_1 \in \mathbb{R}$.*

*ii) $\gamma$ is called an n-helix if the Galilean scalar product of its principal normal vector field $n(s)$ and the constant vector $U$ remain constant for all $s \in I$, that is $\langle n(s), U\rangle = c_2$ for some constant $c_2 \in \mathbb{R}$.*

*iii) $\gamma$ is called a b-helix if the Galilean scalar product of its binormal vector field $b(s)$ and the constant vector $U$ remain constant for all $s \in I$, that is $\langle b(s), U\rangle = c_3$ for some constant $c_3 \in \mathbb{R}$.*

**Definition 5.** *Let $\gamma : I \subset \mathbb{R} \to \mathbb{G}_3$ be a unit speed regular curve and $\delta$ be a vector field along to curve $\gamma$ in $\mathbb{G}_3$. The ruled surfaces*

$$\mathcal{M}^{\varrho} : U \subset \mathbb{R}^2 \to \mathcal{M}^{\varrho} \subset \mathbb{G}_3,\ \mathcal{M}^{\varrho}(s, u) = \gamma(s) + u\delta(s) \tag{11}$$

*is named as* generalized special ruled surfaces *in* $\mathbb{G}_3$ *if their normal vectors are parallel to the vectors* $t(s)$ *or* $n(s)$ *or* $b(s)$. *Considering* $\mu$, $\upsilon, \rho$, *and* $\delta_i (i = 1, 2, 3)$ *smooth functions of s, differentiations of* $\gamma(s)$ *and* $\delta(s)$ *are written by*

$$\gamma'(s) = \mu(s)t(s) + \upsilon(s)n(s) + \rho(s)b(s), \tag{12}$$

*and*

$$\delta(s) = \delta_1(s)t(s) + \delta_2(s)n(s) + \delta_3(s)b(s). \tag{13}$$

In this paper, we consider the Frenet frame $\{t, n, b\}$ of the curve $\gamma$ where $t$ runs along the unit speed regular curve $\gamma = \gamma(s)$, and the curve $\gamma$ has nonzero curvature $\kappa$. On the other hand, we will consider special ruled surfaces $\mathcal{M}^{\varrho}(s, u)$ as follows:

(1) If $\rho(s) = 0$, $\delta_1(s) \neq 0$, $\delta_2(s) = 0$, and $\delta_3(s) = 0$ for every $s \in I$, then the ruled surface $\mathcal{M}^{\varrho}$ is shown as $\mathcal{M}^b$ and is parametrized by

$$\mathcal{M}^b(s, u) = \int (\mu(s)t(s) + \upsilon(s)n(s))ds + u\delta_1(s)t(s). \tag{14}$$

(2) If $\upsilon(s) = 0$, $\delta_2(s) \neq 0$, $\delta_1(s) = 0$, and $\delta_3(s) = 0$ for every $s \in I$, then the ruled surface $\mathcal{M}^{\varrho}$ is shown as $\mathcal{M}^n$ and is parametrized by

$$\mathcal{M}^n(s, u) = \int (\mu(s)t(s) + \rho(s)b(s))ds + u\delta_2(s)n(s). \tag{15}$$

(3) If $\mu(s) = 0$, $\delta_3(s) \neq 0$, $\delta_1(s) = 0$, and $\delta_2(s) = 0$ for every $s \in I$, then the ruled surface $\mathcal{M}^{\varrho}$ is shown as $\mathcal{M}^t$ and is parametrized by

$$\mathcal{M}^t(s, u) = \int (\upsilon(s)n(s) + \rho(s)b(s))ds + u\delta_3(s)b(s). \tag{16}$$

## 4. GCAR whose normal vector is parallel to the vector field $b$

In this section, we consider GCARS whose normal vectors are parallel to the binormal vector field $b$ along the curve $\gamma$. We investigate the singular points of these surfaces and obtain characterizations for the surfaces to exhibit cuspidal edge, swallowtail, and cuspidal butterfly singularities.

**Proposition 1.** *The ruled surface* $\mathcal{M}^b$ *parametrized by Eq (14) is a generalized special ruled surface whose unit normal vector field is the vector field b.*

*Proof.* If we take the partial derivatives of the surface $\mathcal{M}^b(s, u)$ with the parameter $s$ and $u$, we have

$$\left.\begin{array}{c} \frac{\partial}{\partial s}\mathcal{M}^b(s, u) = \left(\mu(s) + u\delta_1'(s)\right)t(s) + \left(\upsilon(s) + u\delta_1(s)\kappa(s)\right)n(s), \\ \frac{\partial}{\partial u}\mathcal{M}^b(s, u) = \delta_1(s)t(s). \end{array}\right\} \tag{17}$$

Therefore, the vector product of above two vector fields can easily calculated by

$$\frac{\partial}{\partial s}\mathcal{M}^b(s, u) \times \frac{\partial}{\partial u}\mathcal{M}^b(s, u) = -\left(\upsilon(s) + u\delta_1(s)\kappa(s)\right)\delta_1(s)b(s), \tag{18}$$

where $\times$ is the vector product in $\mathbb{G}_3$, and $\delta_1(s) \neq 0$. Equation (18) proves that the unit normal vector of $\mathcal{M}^b(s, u)$ is the vector field $b$. □

**Corollary 1.** *The ruled surface $\mathcal{M}^b$ parametrized by Eq (14) is a GCAR if and only if its base curve is a b-helix.*

*Proof.* It is obvious from the above proposition. □

**Proposition 2.** *Let $\gamma : I \subset \mathbb{R} \to \mathbb{G}_3$ be a unit speed regular curve with a nonzero curvature function $\kappa$ in terms of the Frenet frame. The map $\mathcal{M}^b : I \times \mathbb{R} \to\subset \mathbb{G}_3$, given by $\mathcal{M}^b = \int(\mu t + \upsilon n)ds + u\delta_1 t$ , is a wave front.*

*Proof.* The Legendrian mapping over $\mathcal{M}^b$ is written by $L_{\mathcal{M}^b} = (\mathcal{M}^b, \int(\mu t + \upsilon n)ds) : I \times \mathbb{R} \to\subset \mathbb{G}_3$. Then, the Jacobian matrix of $\mathcal{M}^b$ is given as follows:

$$JL_{\mathcal{M}^b} = \begin{bmatrix} (\mu + u\delta_1)\, t + (\upsilon + u\delta_1\kappa)\, n & \mu t + \upsilon n \\ \delta_1 t & 0 \end{bmatrix}.$$

The parametric equation of the surface $\mathcal{M}^b$ implies that $\mu t + \upsilon n \neq 0$ for every $s \in I$. Hence, the Jacobian matrix of $JL_{\mathcal{M}^b}$ has a maximal rank, and then $L_{\mathcal{M}^b}$ is an immersion, that is, $\mathcal{M}^b$ is a wave front. □

**Theorem 1.** *Let $\gamma : I \subset \mathbb{R} \to \mathbb{G}_3$ be a unit speed regular curve with a nonzero curvature function $\kappa$ in terms of the Frenet frame. Then, the singular set of surface $\mathcal{M}^b$ is the set $\left\{(s, \frac{-\upsilon(s)}{\delta_1(s)\kappa(s)}) : s \in I\right\}$.*

*Proof.* Let $\mathcal{M}^b$ be a ruled surface given in Eq (14). By using Eq (18), it is clear that $\left\|\mathcal{M}^b_s(s,u) \times \mathcal{M}^b_u(s,u)\right\| = (\upsilon(s) + u\delta_1(s)\kappa(s))\,\delta_1(s)$. For the singular set of surface $\mathcal{M}^b$, the function $\upsilon(s) + u\delta_1(s)\kappa(s)$ must be zero. This completes the proof. □

**Theorem 2.** *(See [14, 23, 24]) Let $\mathcal{M} : I \times \mathbb{R} \to\subset \mathbb{G}_3$ be a wave front and $p \in U$ be a nondegenerate singular point of $\mathcal{M}$. Then, the following assertions hold:*

*(1) $\mathcal{M}$ at point $p$ is $\mathcal{A}$-equivalent to a **cuspidal edge** if and only if $\eta\lambda(p) \neq 0$.*
*(2) $\mathcal{M}$ at point $p$ is $\mathcal{A}$-equivalent to a **swallowtail** if and only if $\eta\lambda(p) = 0$, and $\eta\eta\lambda(p) \neq 0$.*
*(3) $\mathcal{M}$ at point $p$ is $\mathcal{A}$-equivalent to a **cuspidal butterfly** if and only if $\eta\lambda(p) = 0$, $\eta\eta\lambda(p) = 0$, and $\eta\eta\eta\lambda(p) \neq 0$.*

**Theorem 3.** *Let $\gamma : I \subset \mathbb{R} \to \mathbb{G}_3$ be a unit speed regular curve with a nonzero curvature function $\kappa$ in terms of the Frenet frame. Then, the wave front $\mathcal{M}^b$ has the following characterizations:*

*(1) The wave front $\mathcal{M}^b$ is diffeomorphic to a **cuspidal edge** at the point $p = \{(s, -\upsilon(s)/\delta_1(s)\kappa(s))\}$ if and only if $(-\upsilon(s)/\delta_1(s)\kappa(s))' \neq 0$ for $s \in I$.*
*(2) If $(-\upsilon(s)/\delta_1(s)\kappa(s))' = 0$ for $s \in I$, the wave front $\mathcal{M}^b$ is diffeomorphic to a **swallowtail** at the point $p = \{(s, -\upsilon(s)/\delta_1(s)\kappa(s)\}$ if and only if $(-\upsilon(s)/\delta_1(s)\kappa(s))'' \neq 0$ for $s \in I$.*
*(3) If $(-\upsilon(s)/\delta_1(s)\kappa(s))' = 0$ and $(-\upsilon(s)/\delta_1(s)\kappa(s))'' = 0$ for $s \in I$, the wave front $\mathcal{M}^b$ is diffeomorphic to a **cuspidal butterfly** at the point $p = \{(s, -\upsilon(s)/\delta_1(s)\kappa(s)\}$ if and only if $(-\upsilon(s)/\delta_1(s)\kappa(s))''' \neq 0$ for $s \in I$.*

*Proof.* (1) The density function $\lambda$ of the wave front $\mathcal{M}^b$ is given by $\lambda(s,u) = -(\upsilon(s) + u\delta_1(s)\kappa(s))$, and the null vector field is given as $\eta = \partial/\partial s$. Considering Theorem 2, it is easy to see that

$\mathcal{M}^b$ is diffeomorphic to a **cuspidal edge** at the point $p$ if and only if $\eta\lambda \neq 0$. This implies that $\partial/\partial s\,(-(\upsilon(s) + u\delta_1(s)\kappa(s))) \neq 0$, that is,

$$-(\upsilon'(s) + u\,(\delta_1(s)\kappa(s))') \neq 0. \tag{19}$$

Because $u = -\upsilon(s)/\delta_1(s)\kappa(s)$, Eq (19) can be rewritten as $(-\upsilon(s)/\delta_1(s)\kappa(s))' \neq 0$ for $s \in I$. This completes the proof.

(2) The proof of (1) gives us $\eta\lambda = -(\upsilon'(s) + u\,(\delta_1(s)\kappa(s))')$ and $\eta\eta\lambda = -(\upsilon''(s) + u\,(\delta_1(s)\kappa(s))'')$. At the singular point $p$, $\eta\lambda = \delta_1(s)\kappa(s)(-\upsilon(s)/\delta_1(s)\kappa(s))'$, and $\eta\eta\lambda = -\upsilon''(s) + (\upsilon(s)/\delta_1(s)\kappa(s))\,(\delta_1(s)\kappa(s))''$. From the hypothesis of (2), we know that $(-\upsilon(s)/\delta_1(s)\kappa(s))' = 0$ at $s$. After that, it is clear that $(-\upsilon(s)/\delta_1(s)\kappa(s))'' \neq 0$. This completes the proof.

(3) The proof of (1) gives us $\eta\lambda = -(\upsilon'(s) + u\,(\delta_1(s)\kappa(s))')$, $\eta\eta\lambda = -(\upsilon''(s) + u\,(\delta_1(s)\kappa(s))'')$, and $\eta\eta\eta\lambda = -(\upsilon'''(s) + u\,(\delta_1(s)\kappa(s))''')$. At the singular point $p$, $\eta\lambda = \delta_1(s)\kappa(s)(-\upsilon(s)/\delta_1(s)\kappa(s))'$, $\eta\eta\lambda = -\upsilon''(s) + (\upsilon(s)/\delta_1(s)\kappa(s))\,(\delta_1(s)\kappa(s))''$, and $\eta\eta\eta\lambda = -\upsilon'''(s) + (\upsilon(s)/\delta_1(s)\kappa(s))\,(\delta_1(s)\kappa(s))'''$. From the hypothesis of (3), we know that $(-\upsilon(s)/\delta_1(s)\kappa(s))' = 0$ and $(-\upsilon(s)/\delta_1(s)\kappa(s))'' = 0$ at $s$. After that, it is clear that $(-\upsilon(s)/\delta_1(s)\kappa(s))''' \neq 0$. This completes the proof. □

**Proposition 3.** *The ruled surface $\mathcal{M}^t$ parametrized by Eq (16) is a generalized special ruled surface whose unit normal vector field is the vector field $b$.*

*Proof.* If we take the partial derivatives of the surface $\mathcal{M}^t(s,u)$ with the parameter $s$ and $u$, we have

$$\left.\begin{array}{c} \frac{\partial}{\partial s}\mathcal{M}^t(s,u) = (\upsilon(s) - u\delta_3(s)\tau(s))\,n(s) + \left(\rho(s) + u\delta_3'(s)\right)b(s), \\ \frac{\partial}{\partial u}\mathcal{M}^t(s,u) = \delta_3(s)b(s). \end{array}\right\} \tag{20}$$

Therefore, the vector product of above two vector fields can easily calculated by

$$\frac{\partial}{\partial s}\mathcal{M}^t(s,u) \times \frac{\partial}{\partial u}\mathcal{M}^t(s,u) = (\upsilon(s) - u\delta_3(s)\tau(s))\,\delta_3(s)(1,0,0), \tag{21}$$

where $\times$ is the vector product in $\mathbb{G}_3$, and $\delta_3(s) \neq 0$. Equation (21) proves that the unit normal vector of $\mathcal{M}^t(s,u)$ is the vector field $b$. □

**Corollary 2.** *The ruled surface $\mathcal{M}^t$ parametrized by Eq (16) is a GCAR if and only if its base curve is a b-helix.*

*Proof.* It is obvious from the above proposition. □

**Theorem 4.** *Let $\gamma : I \subset \mathbb{R} \to \mathbb{G}_3$ be a unit speed regular curve with a nonzero torsion function $\tau$ in terms of the Frenet frame. Then, the singular set of surface $\mathcal{M}^t$ is the set $\{(s, \upsilon(s)/\delta_3(s)\tau(s)) : s \in I\}$.*

*Proof.* Let $\mathcal{M}^t$ be a ruled surface given in Eq (16). By using Eq (21), it is clear that $\left\|\mathcal{M}_s^t(s,u) \times \mathcal{M}_u^t(s,u)\right\| = (\upsilon(s) - u\delta_3(s)\tau(s))\,\delta_3(s)$. For the singular set of surface $\mathcal{M}^t$, the function $\upsilon(s) - u\delta_3(s)\tau(s)$ must be zero. This completes the proof. □

**Theorem 5.** *Let $\gamma : I \subset \mathbb{R} \to \mathbb{G}_3$ be a unit speed regular curve with a nonzero torsion function $\tau$ in terms of the Frenet frame. Then, the wave front $\mathcal{M}^t$ has the following characterizations:*

*(1) The wave front $\mathcal{M}^t$ is diffeomorphic to a **cuspidal edge** at the point $p = \{(s, \upsilon(s)/\delta_3(s)\tau(s))\}$ if and only if $(\upsilon(s)/\delta_3(s)\tau(s))' \neq 0$ for $s \in I$.*

*(2) If* $(\upsilon(s)/\delta_3(s)\tau(s))' = 0$ *for* $s \in I$*, the wave front* $\mathcal{M}^t$ *is diffeomorphic to a* ***swallowtail*** *at the point* $p = \{(s, \upsilon(s)/\delta_3(s)\tau(s)\}$ *if and only if* $(\upsilon(s)/\delta_3(s)\tau(s))'' \neq 0$ *for* $s \in I$.

*(3) If* $(\upsilon(s)/\delta_3(s)\tau(s))' = 0$ *and* $(\upsilon(s)/\delta_3(s)\tau(s))'' = 0$ *for* $s \in I$*, the wave front* $\mathcal{M}^t$ *is diffeomorphic to a* ***cuspidal butterfly*** *at the point* $p = \{(s, \upsilon(s)/\delta_3(s)\tau(s))\}$ *if and only if* $(\upsilon(s)/\delta_3(s)\tau(s))''' \neq 0$ *for* $s \in I$.

*Proof.* (1) The density function $\lambda$ of the wave front $\mathcal{M}^t$ is given by $\lambda(s,u) = (\upsilon(s) - u\delta_3(s)\tau(s))$, and the null vector field is given $\eta = \partial/\partial s$. Considering Theorem 2, it is easy to see that $\mathcal{M}^t$ is diffeomorphic to a **cuspidal edge** at the point $p$ if and only if $\eta\lambda \neq 0$. This implies that $\partial/\partial s\left((\upsilon(s) - u\delta_3(s)\tau(s))\right) \neq 0$, that is,

$$\upsilon'(s) - u\left(\delta_3(s)\tau(s)\right)' \neq 0. \tag{22}$$

Because $u = \upsilon(s)/\delta_3(s)\tau(s)$, Eq (22) can be rewritten as $(\upsilon(s)/\delta_3(s)\tau(s))' \neq 0$ for $s \in I$. This completes the proof.

(2) The proof of (1) gives us $\eta\lambda = \upsilon'(s) - u\left(\delta_3(s)\tau(s)\right)'$ and $\eta\eta\lambda = \upsilon''(s) - u\left(\delta_3(s)\tau(s)\right)''$. At the singular point $p$, $\eta\lambda = \delta_3(s)\tau(s)(\upsilon(s)/\delta_3(s)\tau(s))'$, and $\eta\eta\lambda = \upsilon''(s) - (\upsilon(s)/\delta_3(s)\tau(s))\left(\delta_3(s)\tau(s)\right)''$. From the hypothesis of (2), we know that $(\upsilon(s)/\delta_3(s)\tau(s))' = 0$ at $s$. After that, it is clear that $(\upsilon(s)/\delta_3(s)\tau(s))'' \neq 0$. This completes the proof.

(3) The proof of (1) gives us $\eta\lambda = \upsilon'(s) - u\left(\delta_3(s)\tau(s)\right)'$, $\eta\eta\lambda = \upsilon''(s) - u\left(\delta_3(s)\tau(s)\right)''$, and $\eta\eta\eta\lambda = \upsilon'''(s) - u\left(\delta_3(s)\tau(s)\right)'''$. At the singular point $p$, $\eta\lambda = \delta_3(s)\tau(s)(\upsilon(s)/\delta_3(s)\tau(s))'$, $\eta\eta\lambda = \upsilon''(s) - (\upsilon(s)/\delta_3(s)\tau(s))\left(\delta_3(s)\tau(s)\right)''$, and $\eta\eta\eta\lambda = \upsilon'''(s) - (\upsilon(s)/\delta_3(s)\tau(s))\left(\delta_3(s)\tau(s)\right)'''$. From the hypothesis of (3), we know that $(\upsilon(s)/\delta_3(s)\tau(s))' = 0$ and $(\upsilon(s)/\delta_3(s)\tau(s))'' = 0$ at $s$. After that, it is clear that $(\upsilon(s)/\delta_3(s)\tau(s))''' \neq 0$. This completes the proof. □

**Corollary 3.** *The GCARS* $\mathcal{M}^n$ *whose normal vector is parallel to the principal normal vector field n has no singular points.*

*Proof.* Taking the partial derivatives of the surface $\mathcal{M}^n(s,u)$ with respect to $s$ and $u$, the cross-product yields components along $b$ and $(1,0,0)$. Because $b \neq 0$, and the surface definition requires $\delta_2 \neq 0$, the expression cannot completely vanish. Thus, no singularities exist unless $\mu(s) = 0$. □

## 5. Examples

In this section, we give some examples of $\mathcal{M}^b(s,u)$, a constant-angle ruled surface with singularities using the Mathematica Programme.

**Example 1.** *We are given a general helix*

$$\gamma(s) = \left(s, \frac{e^{-s}}{25}\left(-3\cos 2s - 4\sin 2s\right), \frac{e^{-s}}{25}\left(4\cos 2s - 3\sin 2s\right)\right).$$

*The Frenet frame* $\{t(s), n(s), b(s)\}$ *can be calculated as follows:*

$$t(s) = \gamma'(s) = \left(1, \frac{e^{-s}}{5}\left(2\sin 2s - \cos 2s\right), -\frac{e^{-s}}{5}\left(\sin 2s + 2\cos 2s\right)\right),$$

$$n(s) = \frac{1}{\kappa(s)}\left(0, y''(s), z''(s)\right) = \left(0, \cos 2s, \sin 2s\right),$$

$$b(s) = \frac{1}{\kappa(s)}\left(0, -z''(s), y''(s)\right) = \left(0, -\sin 2s, \cos 2s\right),$$

*where* $\kappa(s) = e^{-s}, \tau(s) = 2$, *and* $\times$ *denote the vector product. Therefore, we can write the constant-angle ruled surface as*

$$\mathcal{M}^b(s,u) = \left(\mathcal{M}_1^b(s,u), \mathcal{M}_2^b(s,u), \mathcal{M}_3^b(s,u)\right),$$

*and we get a constant-angle ruled surfaces' components and its singularities as follows:*

$$\mathcal{M}^b(s,u) = \begin{cases} \mathcal{M}_1^b(s,u) = \int \mu(s)\, ds + u\delta_1(s), \\ \mathcal{M}_2^b(s,u) = \int \left(\mu(s)\left(\frac{e^{-s}}{5}(2\sin 2s - \cos 2s)\right) + \upsilon(s)\cos 2s\right) ds + u\delta_1(s)\left(\frac{e^{-s}}{5}(2\sin 2s - \cos 2s)\right), \\ \mathcal{M}_3^b(s,u) = \int \left(\mu(s)\left(-\frac{e^{-s}}{5}(\sin 2s + 2\cos 2s)\right) + \upsilon(s)\sin 2s\right) ds + u\delta_1(s)\left(-\frac{e^{-s}}{5}(\sin 2s + 2\cos 2s)\right). \end{cases}$$

*(i) If we get* $\mu(s) = s + 1$ *in* $\mathcal{M}^b(s,u) = \left(\mathcal{M}_1^b(s,u), \mathcal{M}_2^b(s,u), \mathcal{M}_3^b(s,u)\right)$,

$$\mathcal{M}^b(s,u) = \int ((s+1)\left(1, \frac{e^{-s}}{5}(2\sin 2s - \cos 2s), -\frac{e^{-s}}{5}(\sin 2s + 2\cos 2s)\right) + \upsilon(s)(0, \cos 2s, \sin 2s))ds + \frac{(s+1)}{\kappa(s)}\left(1, \frac{e^{-s}}{5}(2\sin 2s - \cos 2s), -\frac{e^{-s}}{5}(\sin 2s + 2\cos 2s)\right).$$

*(ii) If we get* $\mu(s) = \sin(s^2 + 1)$ *in* $\mathcal{M}^b(s,u) = \left(\mathcal{M}_1^b(s,u), \mathcal{M}_2^b(s,u), \mathcal{M}_3^b(s,u)\right)$,

$$\mathcal{M}^b(s,u) = \int ((\sin(s^2+1))\left(1, \frac{e^{-s}}{5}(2\sin 2s - \cos 2s), -\frac{e^{-s}}{5}(\sin 2s + 2\cos 2s)\right) + \upsilon(s)(0, \cos 2s, \sin 2s))ds + \frac{\sin(s^2+1)}{\kappa(s)}\left(1, \frac{e^{-s}}{5}(2\sin 2s - \cos 2s), -\frac{e^{-s}}{5}(\sin 2s + 2\cos 2s)\right).$$

*(iii) If we get* $\mu(s) = s^3 + 1$ *in* $\mathcal{M}^b(s,u) = \left(\mathcal{M}_1^b(s,u), \mathcal{M}_2^b(s,u), \mathcal{M}_3^b(s,u)\right)$,

$$\mathcal{M}^b(s,u) = \int ((s^3+1)\left(1, \frac{e^{-s}}{5}(2\sin 2s - \cos 2s), -\frac{e^{-s}}{5}(\sin 2s + 2\cos 2s)\right) + \upsilon(s)(0, \cos 2s, \sin 2s))ds + \frac{s^3+1}{\kappa(s)}\left(1, \frac{e^{-s}}{5}(2\sin 2s - \cos 2s), -\frac{e^{-s}}{5}(\sin 2s + 2\cos 2s)\right),$$

*where* $\upsilon(s) = 1$.

*Thus, we get three graphs, which are shown in Figure 1: (a) (the red line is the* cuspidal edge*, where* $\mu(s) = s + 1$*, and* $\upsilon(s) = 1$*), (b) (the red line is the* swallowtail*, where* $\mu(s) = \sin(s^2 + 1)$*, and* $\upsilon(s) = 1$*) and (c) (the red line is the* cuspidal butterfly*, where* $\mu(s) = s^3 + 1$*, and* $\upsilon(s) = 1$*), respectively.*

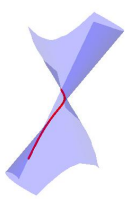

**(a)** Cuspidal edge

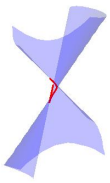

**(b)** Swallowtail

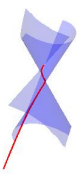

**(c)** Cuspidal butterfly

**Figure 1.** The constant-angle ruled surface $\mathcal{M}^b(s,u)$.

**Example 2.** *We are given a circular helix*

$$\gamma(s) = (s, \cos s, \sin s).$$

*The Frenet frame* $\{t(s), n(s), b(s)\}$ *can be calculated as follows:*

$$t(s) = \gamma'(s) = (1, -\sin s, \cos s),$$
$$n(s) = \frac{1}{\kappa(s)}(0, y''(s), z''(s)) = (0, -\cos s, -\sin s),$$
$$b(s) = \frac{1}{\kappa(s)}(0, -z''(s), y''(s)) = (0, \sin s, -\cos s),$$

*where* $\kappa(s) = 1, \tau(s) = 1$, *and* $\times$ *denote the vector product. Therefore, we can write the constant-angle ruled surface as*

$$\widetilde{\mathcal{M}}^b(s,u) = \left(\widetilde{\mathcal{M}}_1^b(s,u), \widetilde{\mathcal{M}}_2^b(s,u), \widetilde{\mathcal{M}}_3^b(s,u)\right),$$

*and we get a constant-angle ruled surfaces' components and its singularities as follows:*

$$\widetilde{\mathcal{M}}^b(s,u) = \begin{cases} \widetilde{\mathcal{M}}_1^b(s,u) &= \int \mu(s)\,ds + u\delta_1(s), \\ \widetilde{\mathcal{M}}_2^b(s,u) &= \int (\mu(s)(-\sin s) + \upsilon(s)(-\cos s))\,ds + u\delta_1(s)(-\sin s), \\ \widetilde{\mathcal{M}}_3^b(s,u) &= \int (\mu(s)\cos s + \upsilon(s)(-\sin s))\,ds + u\delta_1(s)\cos s. \end{cases}$$

*(i) If we get* $\mu(s) = s + 1$ *in* $\widetilde{\mathcal{M}}^b(s,u) = \left(\widetilde{\mathcal{M}}_1^b(s,u), \widetilde{\mathcal{M}}_2^b(s,u), \widetilde{\mathcal{M}}_3^b(s,u)\right)$,

$$\widetilde{\mathcal{M}}^b(s,u) = \int ((s+1)(1, -\sin s, \cos s) + \upsilon(s)(0, -\cos s, -\sin s))\,ds + \frac{(s+1)}{\kappa(s)}(1, -\sin s, \cos s).$$

*(ii) If we get* $\mu(s) = s^2 + 1$ *in* $\widetilde{\mathcal{M}}^b(s,u) = \left(\widetilde{\mathcal{M}}_1^b(s,u), \widetilde{\mathcal{M}}_2^b(s,u), \widetilde{\mathcal{M}}_3^b(s,u)\right)$,

$$\widetilde{\mathcal{M}}^b(s,u) = \int \left(\left(s^2+1\right)(1, -\sin s, \cos s) + \upsilon(s)(0, -\cos s, -\sin s)\right)ds + \frac{(s^2+1)}{\kappa(s)}(1, -\sin s, \cos s).$$

*(iii) If we get* $\mu(s) = s^3 + 1$ *in* $\widetilde{\mathcal{M}}^b(s,u) = \left(\widetilde{\mathcal{M}}_1^b(s,u), \widetilde{\mathcal{M}}_2^b(s,u), \widetilde{\mathcal{M}}_3^b(s,u)\right)$,

$$\widetilde{\mathcal{M}}^b(s,u) = \int \left(\left(s^3+1\right)(1, -\sin s, \cos s) + \upsilon(s)(0, -\cos s, -\sin s)\right)ds + \frac{(s^3+1)}{\kappa(s)}(1, -\sin s, \cos s),$$

*where* $\upsilon(s) = 1$.

*Thus, we get three graphs, which are shown in Figure 2: (a) (the red line is the* cuspidal edge, *where* $\mu(s) = s + 1$, *and* $\upsilon(s) = 1$*), (b) (the red line is the* swallowtail, *where* $\mu(s) = s^2 + 1$, *and* $\upsilon(s) = 1$*) and (c) (the red line is the* cuspidal butterfly, *where* $\mu(s) = s^3 + 1$, *and* $\upsilon(s) = 1$*), respectively.*

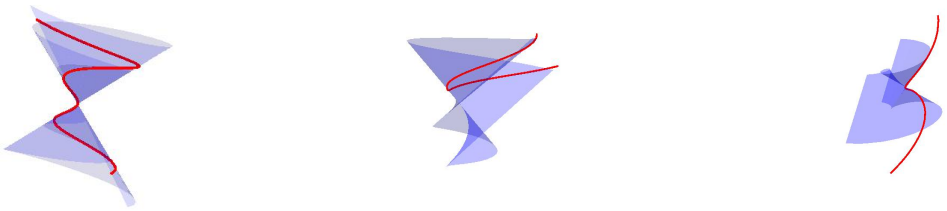

**(a)** Cuspidal edge **(b)** Swallowtail **(c)** Cuspidal butterfly

**Figure 2.** The constant-angle ruled surface $\widetilde{\mathcal{M}}^b(s,u)$.

## 6. Conclusions

In this study, a generalized version of constant-angle ruled surfaces constructed using the Frenet frame in 3-dimensional Galilean space ($\mathbb{G}_3$) was obtained and analyzed in detail. We defined generalized special ruled surfaces by systematically considering cases where the surface normal vectors are parallel to the tangent ($t$), principal normal ($n$), or binormal ($b$) vector fields of the base curve, and we presented various criteria regarding the locus of singular points for these surfaces.

Our analysis focused specifically on the singularities of general constant angle ruled surfaces ($\mathcal{M}^b$ and $\mathcal{M}^t$) whose normal vectors are parallel to the binormal and tangent vector fields, respectively. Through rigorous mathematical investigation, the singular set for the $\mathcal{M}^b$ surface was explicitly characterized as $\{(s, -v(s)/\delta_1(s)\kappa(s)) : s \in I\}$. Clear conditions were established under which both surface types ($\mathcal{M}^b$ and $\mathcal{M}^t$) exhibit cuspidal edge, swallowtail, and cuspidal butterfly singularities. Conversely, we concluded that the general constant-angle ruled surface $\mathcal{M}^n$, whose normal vector is parallel to the principal normal ($n$) vector field, possesses no singular points.

To support these theoretical findings, applications involving general and circular helix examples were modeled using Mathematica in the final section. Through these examples, the cuspidal edge, swallowtail, and cuspidal butterfly singularities on the investigated surfaces were successfully visualized, clearly demonstrating the geometric implications of our theoretical calculations.

These mathematical generalizations and singularity analyses have the potential to benefit various applied sciences beyond differential geometry. In a physical context, Galilean space is critical for expressing classical physics principles, such as velocity, momentum, kinetic energy, and laws of motion, and for modeling the limit transition from the special theory of relativity to classical mechanics. Therefore, our findings regarding surface singularities in this space may facilitate more accurate modeling of kinematic and dynamic systems in non-relativistic physics. Furthermore, helical structures have broad physical applications in biology and nanotechnology, appearing in DNA double helices, carbon nanotubes, nanosprings, bacterial flagella, and collagen structures. Consequently, the theoretical framework established in this study could serve as a solid foundation for developing advanced, high-precision algorithms to investigate hyperhelices in fractal geometry or to define tool paths for robotic kinematic motions via computer simulations.

## Author contributions

Ümit Tokeşer and Seda Nur Ídrísoğlu: Conceptualization, Methodology, Validation, Writing-original draft, Writing-review & editing. Both authors contributed equally to this work. Both authors have read and approved the final version of the manuscript for publication.

## Use of Generative-AI tools declaration

The authors confirm that the content of this article is entirely their own work. Artificial intelligence (AI) tools were not used in the mathematical analysis or results.

## Conflict of interest

The authors declare no conflict of interest.

## References


1. N. Chouaieb, A. Goriely, J. Maddocks, Helices, *Proc. Natl. Acad. Sci. U.S.A.*, **103** (2006), 9398–9403. https://doi.org/10.1073/pnas.0508370103
2. A. Lucas, P. Lambin, Diffraction by DNA, carbon nanotubes and other helical nanostructures, *Rep. Prog. Phys.*, **68** (2005), 1181. https://doi.org/10.1088/0034-4885/68/5/R05
3. J. Watson, F. Crick, Genetical implications of the structure of deoxyribonucleic acid, *JAMA*, **236** (1993), 1967–1969. https://doi.org/10.1001/jama.1993.03500150079031
4. C. Toledo-Suárez, On the arithmetic of fractal deimension using hyperhelices, *Chaos Solition. Fract.*, **39** (2009), 342–349. https://doi.org/10.1016/j.chaos.2007.01.095
5. X. Yang, High accuracy approximation of helices by quintic curve, *Comput. Aided Geom. D.*, **20** (2003), 303–317. https://doi.org/10.1016/S0167-8396(03)00074-8
6. M. Külahci, Characterizations of a helix in the Pseudo-Galilean space $\mathbb{G}_3^1$, *Int. J. Phys. Sci.*, **5** (2010), 1438–1442.
7. A. Ali, Position vectors of curves in the Galilean space $\mathbb{G}_3$, *Mat. Vesnik*, **64** (2012), 200–210.
8. E. Nešović, U. Öztürk, E. Öztürk, On $T$-slant, $N$-slant and $B$-slant helices in Galilean space $\mathbb{G}_3$, *J. Dyn. Syst. Geom. The.*, **16** (2018), 187–199. https://doi.org/10.1080/1726037X.2018.1436271
9. U. Öztürk, E. Nešović, E. Öztürk, On $T$-slant, $N$-slant and $B$-slant helices in Pseudo-Galilean space $\mathbb{G}_3^1$, *Filomat*, **32** (2018), 245–253. https://doi.org/10.2298/FIL1801245O
10. A. Ogrenmis, M. Ergut, M. Bektas, On the helices in the Galilean space $\mathbb{G}_3$, *Iran. J. Sci. Technol. A*, **31** (2007), 177–181.
11. B. Yilmaz, S. Metin, I. Gok, Y. Yayli, Harmonic curvature functions of some special curves in Galilean 3-space, *Honam Math. J.*, **41** (2019), 301–319.
12. Z. Erjavec, On generalization of helices in the Galilean and the Pseudo-Galilean space, *Journal of Mathematics Research*, **6** (2014), 39–50. https://doi.org/10.5539/jmr.v6n3p39
13. B. Divjak, Z. Milin-Šipuš, Special curves on ruled surfaces in Galilean and pseudo-Galilean spaces, *Acta Math. Hung.*, **98** (2002), 203–215. https://doi.org/10.1023/a:1022821824927
14. A. Alghanemi, S. Alofi, On the singularities of gaussian rectifying surface and special curves, *J. Math. Anal.*, **9** (2018), 48–58.
15. E. Solouma, S. Saber, H. Baskonus, Exploring harmonic evolute geometries derived from tubular surfaces in Minkowski 3-space using the RM Darboux frame, *Mathematics*, **13** (2025), 2329. https://doi.org/10.3390/math13152329
16. E. Solouma, S. Saber, M. Marin, H. Baskonus, Geometric invariants and evolution of RM Hasimoto surfaces in Minkowski 3-space $\mathbb{E}_1^3$, *Mathematics*, **13** (2025), 3420. https://doi.org/10.3390/math13213420

17. M. Messaoudi, E. Solouma, M. Alshehri, A. Aljohani, M. Marin, Lorentzian structure and curvature analysis of osculating type-2 ruled surfaces via the type-2 bishop frame, *Mathematics*, **13** (2025), 3464. https://doi.org/10.3390/math13213464
18. E. Solouma, I. Al-Dayel, M. Khan, Y. Lazer, Characterization of imbricate-ruled surfaces via rotation minimizing Darboux frame in Minkowski 3-space, *AIMS Mathematics*, **9** (2024), 13028–13042. https://doi.org/10.3934/math.2024635
19. E. Solouma, I. Al-Dayel, M. Abdelkawy, Ruled surfaces and their geometric invariants via the orthogonal modified frame in Minkowski 3-space, *Mathematics*, **13** (2025), 940. https://doi.org/10.3390/math13060940
20. M. Bin-Asfour, G. Alhamzi, E. Solouma, S. Saber, A unified rotation-minimizing Darboux framework for curves and relativistic ruled surfaces in Minkowski three-space, *Axioms*, **15** (2026), 207. https://doi.org/10.3390/axioms15030207
21. T. Şahin, M. Yilmaz, On singularities of the Galilean spherical Darboux ruled surface of a space curve in $\mathbb{G}_3$, *Ukr. Math. J.*, **62** (2011), 1597–1610. https://doi.org/10.1007/s11253-011-0452-9
22. A. Ali, A constant angle ruled surfaces, *International Journal of Geometry*, **7** (2018), 69–80.
23. M. Kokubu, W. Rossman, K. Saji, M. Umehara, K. Yamada, Singularities of flat fronts in hyperbolic 3-space, *Pac. J. Math.*, **221** (2005), 303–351. https://doi.org/10.2140/pjm.2005.221.303
24. S. Izumiya, K. Saji, The mandala of Legendrian dualities for pseudo-spheres of Lorentz-Minkowski space and spacelike surfaces, *J. Singul.*, **2** (2010), 21–127. https://doi.org/10.5427/jsing.2010.2g


AIMS Press